Registry-dependent interlayer potential for graphitic systems

Aleksey N. Kolmogorov and Vincent H. Crespi
Department of Physics, The Pennsylvania State University, 104 Davey Lab, University Park, Pennsylvania 16802-6300, USA
(Received 21 February 2005; published 27 June 2005)

Standard applications of density functional theory do not adequately describe the exfoliation energy of graphite. In fact, the local density approximation (LDA) and generalized gradient approximation (GGA) are in qualitative disagreement: the LDA binds at the experimental lattice constant, whereas the GGA does not. However, the variation in the energy under interlayer shifts, due predominantly to the overlap of π orbitals (not dispersion interactions), is nearly identical in these approximations. We combine these results with experimental information on the exfoliation energy to create an improved registry-dependent classical potential for the interlayer interaction in graphitic structures.

DOI: 10.1103/PhysRevB.71.235415 PACS number(s): 68.35.−p, 71.15.Nc, 71.15.Mb, 61.50.Lt

The discovery of carbon nanotubes[1] has opened up the possibility of building electronic and mechanical carbon-based devices at the nanoscale. Although made from strongly bound sp^2 carbon networks, nanotubes interact only weakly with one another. But it is this interaction that will define the function of nanodevices such as bearings or motors[2–5] or mechanisms to distinguish nanotubes by helical angle via interaction with graphite substrates.[6,7] Large-scale simulations of nanomechanical systems are beyond the capabilities of modern quantum mechanical methods, so empirical potentials must be applied. A pairwise Lennard-Jones (LJ) potential can describe the overall cohesion between graphene layers,[8] but it is much too smooth to describe variations in the relative alignment of adjacent layers. To account for this registry dependence (henceforth referred to as *corrugation*) and to realistically simulate the interaction of graphitic interfaces containing thousands of atoms, we have developed an empirical interlayer potential using the latest experimental and theoretical knowledge about the interaction.

The cohesion in layered graphitic structures is a combination of long-ranged van der Waals (vdW) and short-ranged orbital overlap contributions. The vdW coupling is missing in the local density (LDA) and the generalized gradient approximations (GGA), so these methods do not adequately describe the interlayer cohesion in graphite[8–10] (although the LDA does yield nearly the correct interlayer spacing and a binding energy within a factor of 2 of experiment). An important step toward a more complete model has been taken by Rydberg *et al.*,[9] who included the long-ranged vdW coupling as a nonlocal functional of the charge density, incorporating the polarizability of the graphitic layers. For calculation of the dielectric function the charge density was smoothed in plane, which is a good approximation for the description of the total interlayer binding. For revealing the corrugation from the vdW term a more careful treatment of the dielectric response is required.[11,12] Palser has suggested that the difference in the binding energy for different forms of graphite calculated in the LDA (Ref. 13) gives a qualitative measure for the corrugation in graphitic structures which can be used to guide the construction of an empirical tight-binding-plus-dispersion model of the interlayer interaction.[14] Here we suggest that, although the absolute cohesion is not properly described in the LDA or GGA, the corrugation appears to be much more sound than previously suspected. We combine this result with experimental data on the exfoliation energy to create a classical potential that can describe the corrugation in graphitic systems with reasonable accuracy.

Experimental measurements are usually done on natural graphite, which is a mixture of ordered (*AB* stacked, *ABC* stacked) and disordered (turbostratic) layered structures,[13] shown in Fig. 1. The equilibrium interlayer distance[15] (3.34 Å) and *c*-axis compressibility[16] (2.7×10^{-12} cm^2/dyn) of graphite can be measured with good accuracy. The absolute interlayer binding energy (i.e., exfoliation energy) is harder to extract; only a handful of results exist in the literature. A heat-of-wetting experiment by Girifalco and Ladd gives an exfoliation energy of 43 meV/atom.[17] A microscopic determination of the interlayer binding through study of collapsed nanotubes yields 35 ± 10 meV/atom.[18] Later experiments on thermal desorption of polyaromatic hydrocarbons give a larger binding energy of 52 ± 5 meV/atom.[19] These discrepancies might arise from different structural constraints in the three systems. Conjugated molecules on a graphite substrate form the least constrained system, with both rotational and translational degrees of freedom. Thus, the molecules can exploit finite-size effects to find the best registration with the substrate and achieve higher cohesion. In contrast, collapsed nanotubes are highly constrained due to circumferential continuity. The opposite inner surfaces of a chiral nanotube are skewed, which results in a suboptimal turbostraticlike interlayer registration and a weaker cohesion when collapsed. Unfortunately, the experimental values quoted above are not accurate enough to extract a quantitative measure of the corrugation.[20] However, the increase in the interlayer spacing of bulk turbostratic graphite due to the random orientation of graphene layers has been measured: later we will use this information as an independent test of our potential. Experimental data on *AA* stacking [Fig. 1(a)] would be very helpful, but this form has not been observed.

Because there are no direct experimental data on corrugation in graphite, we investigate what information can be obtained theoretically. We perform first-principle calculations using[21–24] VASP with ultrasoft pseudopotentials[25] and

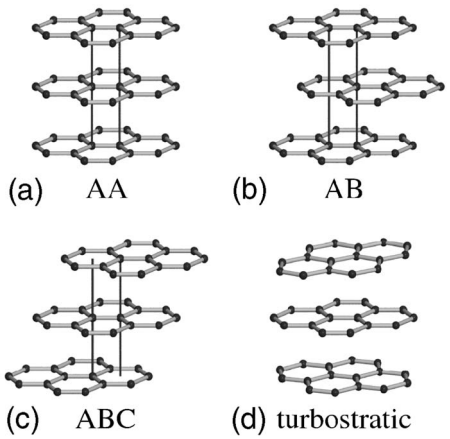

FIG. 1. Different stackings of graphite.

exchange-correlation functionals as parametrized by Perdew and Zunger[26] for the LDA and Perdew, Burke, and Ernzerhof[27] for the GGA. The scale of most of the effects we study is a few meV/atom, so high accuracy is required. We use an energy cutoff of 358 eV with a sufficient number of special k points[28] to ensure convergence. Figure 2 illustrates how the LDA and GGA functionals describe the interplanar binding of graphite. The LDA finds the right interlayer spacing for *AB* stacking, but underestimates the exfoliation energy by a factor of 2 and overestimates the compressibility. The GGA shows no binding at all at physically meaningful spacings. The exfoliation energies are strongly affected by the locality of the exchange-correlation functionals used in the two approximations. First, the electrodynamic coupling between the layers is missing, which results in the weaker binding. Second, the two methods employ different approximate forms for the exchange-correlation functional; they differ the most in regions of rapidly varying charge density. Because a layered structure such as graphite (or a single layer of graphene) has a strongly varying charge density, the LDA and GGA functionals produce very different results for the absolute binding, as is well known in the literature.

However, Fig. 2(b) shows that even without nonlocal corrections the energy *difference* between the *AA* and *AB* stackings of graphite at constant interlayer spacing is essentially identical in LDA and GGA: 15 meV/atom at 3.34 Å spacing. The result is also independent of the details of the calculations: we find similar values for the corrugation when using a hard pseudopotential,[29] an ultrasoft pseudopotential,[25] or projector-augmented waves,[30] if sufficient k points are used for tight convergence. These results are also close to a previously reported value, 17 meV/atom, obtained in a hard-pseudopotential calculation by Charlier *et al.*[13] The consistency of these values suggests that errors cancel when two bulk structures are compared directly. This is not surprising, since the LDA and GGA describe relative energies of systems with similar charge densities better than absolute exfoliation or atomization energies. Nevertheless, the LDA and GGA functionals are still missing the nonlocal correlations. We investigate the errors associated with the local treatment of the correlation effects in the following way.

First, we analyze how much the nonlocal correlations

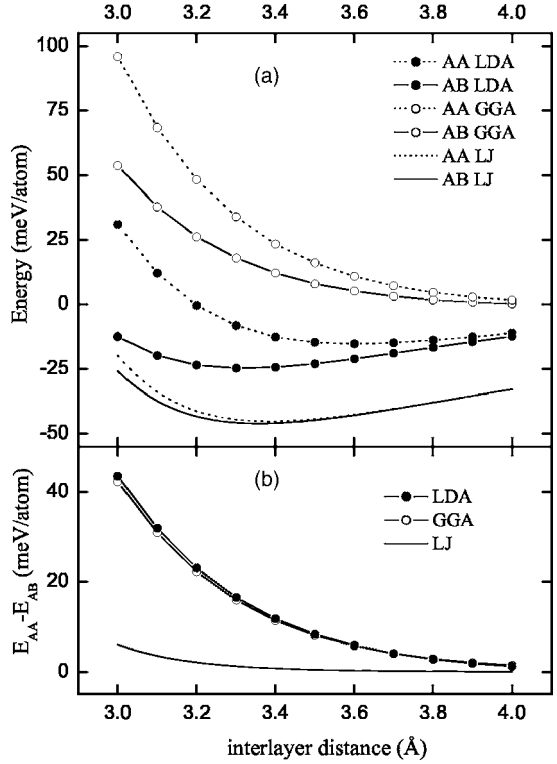

FIG. 2. (a) Interlayer energy in graphite in the local-density approximation (LDA), generalized gradient approximation (GGA), and Lennard-Jones (LJ) treatment for *AA* and *AB* stackings of graphite. (b) The energy difference between *AA* and *AB* stackings of graphite as a function of the interlayer distance.

would contribute to the total corrugation if they were indeed properly calculated. A quick estimate of this contribution can be made by considering the vdW coupling as a pairwise interaction between atoms with an r^{-6} dependence. We take this term as in the LJ potential:[31]

$$V_{LJ}(r) = 4\epsilon\left[-\left(\frac{\sigma}{r}\right)^6 + \left(\frac{\sigma}{r}\right)^{12}\right], \tag{1}$$

where for graphene/graphene ϵ=2.39 meV and σ=3.41 Å. We find that while the vdW coupling is an essential part of the total interlayer binding, it is very weakly dependent on the interlayer alignment. The energy difference between the *AA* and *AB* stacked graphite due to the r^{-6} dispersion term in the Lennard-Jones interaction is about 0.3 meV/atom, which is just 2% of the LDA value. For this long-ranged term the interaction energy is an average over a large area and turns out to depend more on the distance between the layers than on their relative alignment. Long-ranged correlations could play a somewhat bigger role in the corrugation against sliding for structures of lower dimensionality (nanotubes, fullerenes) due to less efficient averaging. Another possible increase in the vdW contribution to corrugation could be caused by local field effects, as a careful study of the polarizability anisotropy in graphite suggests.[11] To get an idea of how this would affect the corrugation we use a classical model of Crowell and Brown[32] (CB), who introduced the

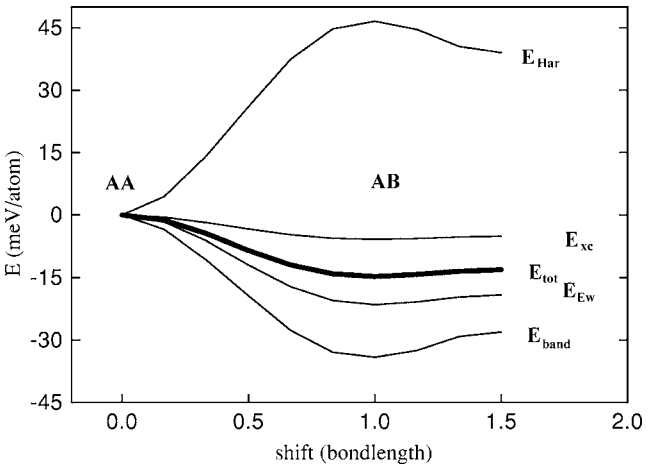

FIG. 3. Contributions to corrugation against sliding for two graphene sheets 3.34 Å apart calculated in the LDA with VASP. The GGA gives very close results. From top to bottom: Hartree, exchange-correlation, total, Ewald, and band-structure energies.

dependence of the dispersion forces on the anisotropic polarizability of graphitic layers in the following way:

$$V_{CB}(r) = -(E_C/8)[(P_\parallel - P_\perp)^2(1-3\cos^2\theta)^2 + 6P_\perp(P_\parallel - P_\perp)\cos^2\theta + 2P_\perp(P_\parallel + 2P_\perp)]r^{-6} + \gamma_R\left(\frac{\sigma_{CC}}{r}\right)^{12}. \quad (2)$$

θ is the angle between the c axis and a line joining a pair of noncoplanar carbon atoms. $P_\parallel$ and $P_\perp$ denote polarizabilities parallel and perpendicular to the c axis, respectively. The angular dependence increases the corrugation from the vdW coupling to just 0.7 meV/atom, which thus remains much smaller compared to the LDA value of 15 meV/atom.

Second, we break down the total corrugation in our LDA and GGA calculations into individual contributions from different terms and plot them in Fig. 3. The exchange-correlation term should be the least accurate, since the functional for the nonlocal correlations is not known exactly. However, the magnitude of its variation under sliding is the smallest of the four. The local description of the correlation also affects the accuracy of the other terms, but weakly and indirectly through the charge density.

To sum up, our tests suggest that corrugation comes primarily from short-ranged, exponentially decaying orbital overlaps. The corrugation arising from this contribution is adequately described in the local DFT approximations, and by shifting or rotating one layer with respect to the other one can extract physically meaningful information about the interaction.

Now we will check how existing empirical potentials compare against the corrugation calculated in the LDA (so far we have examined only the dispersion term in these potentials, not including the short-ranged repulsion). The widely used Lennard-Jones pair potential[31] given in Eq. (1) reproduces the equilibrium spacing, cohesion, and compressibility of graphite along the c axis [see Fig. 2(a)]. This justifies its popularity for the description of the averaged interlayer interaction. But Fig. 2(b) reveals that the LJ potential is much too smooth under interlayer shift: at the equilibrium spacing the corrugation is less than 10% of that found in the LDA. The CB potential underestimates the corrugation in a similar way: for both potentials corrugation comes predominantly from the more singular r^{-12} repulsive term. The real π overlap between layers is anisotropic and cannot be described in a natural way by the single length scale of a Lennard-Jones potential. If the potential is isotropic (i.e., depends only on the distance between pairs of atoms), then the experimental c-axis compressibility and the corrugation cannot be fitted simultaneously.

To decouple these quantities one must distinguish between in-plane and out-of-plane directions. We have designed an improved classical potential to do this. The potential contains an r^{-6} vdW attraction and an exponentially decaying repulsion due to the interlayer wave-function overlap. To reflect the directionality of the overlap we introduce a function f which rapidly decays with the transverse distance ρ:

$$V(\mathbf{r}_{ij},\mathbf{n}_i,\mathbf{n}_j) = e^{-\lambda(r_{ij}-z_0)}[C + f(\rho_{ij}) + f(\rho_{ji})] - A\left(\frac{r_{ij}}{z_0}\right)^{-6},$$

$$\rho_{ij}^2 = r_{ij}^2 - (\mathbf{n}_i\mathbf{r}_{ij})^2,$$

$$\rho_{ji}^2 = r_{ij}^2 - (\mathbf{n}_j\mathbf{r}_{ij})^2,$$

$$f(\rho) = e^{-(\rho/\delta)^2}\sum C_{2n}(\rho/\delta)^{2n}. \quad (3)$$

The energy is measured in meV, and the vector $\mathbf{n}_k$ $(k=i,j)$ is normal to the sp^2 plane in the vicinity of atom k. The proper definition of the surface normal (for a plane composed of discrete atoms) is important. We have previously proposed a registry-dependent potential,[33] or RDP0, in which the in-plane and out-of-plane directions were defined assuming global knowledge about the symmetry of the system. That potential is in fair agreement with the LDA data on corrugation for flat and curved surfaces, but this global definition of the normals prohibits its application to structures of arbitrary geometry. In general, the orientation of the p_z orbital on an arbitrary sp^2 carbon site is determined by the local environment, not the global symmetry. Therefore we now define the normal at a given atom using only a small patch of neighboring atoms.

The simplest definition of normal uses the three nearest neighbors. For example, one can average the three normalized cross products of the displacement vectors to the nearest neighbors. However, since π bonding is relatively delocalized, a broader sampling of the local neighborhood may give a better normal. For nanotubes, the "local" normal defined above tends to tilt toward the center of one of the neighboring hexagons, especially for smaller-diameter tubes. An alternative definition includes second neighbors as well: after the local normals are found, the direction of a "semilocal" normal can be calculated as

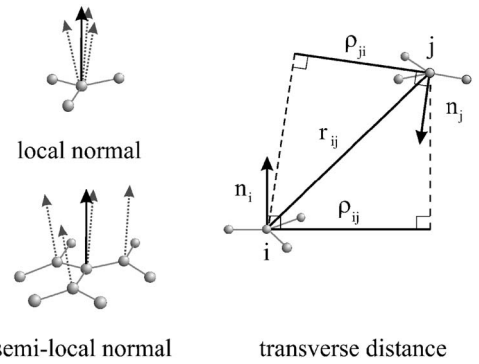

FIG. 4. Definitions of the normal vector on an sp^2 carbon site and the transverse distances between two atoms.

$$\mathbf{n}_i \propto a\mathbf{n}_i^{loc} + \mathbf{n}_{i1}^{loc} + \mathbf{n}_{i2}^{loc} + \mathbf{n}_{i3}^{loc} \tag{4}$$

where $\mathbf{n}_{i1}^{loc}$, $\mathbf{n}_{i2}^{loc}$, and $\mathbf{n}_{i3}^{loc}$ are local normals for the first neighbors of atom i. The parameter a interpolates between the two cases ($a=\infty$ corresponds to the local normals). Once a normal is defined, the transverse distance is the projection of the radius vector onto the plane perpendicular to the normal (see Fig. 4). We will assess each of these definitions, and find that while the semilocal normal yields a more accurate potential overall, the local normal yields a more consistent overestimation of the corrugation.

Having defined the normals, we adjust the seven parameters in Eq. (3) with a conjugate gradient technique to minimize the least square error. Our training set is a careful weighing of experimental and theoretical results. The compressibility (2.7×10^{-12} cm^2/dyn) and the equilibrium interlayer spacing (3.34 Å) of *AB* stacking are weighed the most and closely match the experimental values. The experimental interlayer binding energy for natural graphite is less accurate; our potential gives 48 meV/atom. For the corrugation we take the LDA data on sliding for graphene/graphene [shown in Fig 2(b)] and nanotube/graphene [for (5,5) and (10,0) nanotubes as shown in Fig. 5] interfaces. The resulting parameters are $C_0=15.71$, $C_2=12.29$, $C_4=4.933$, $C=3.030$, $\delta=0.578$ Å, $\lambda=3.629$ Å^{-1}, $A=10.238$; the scaling factor $z_0=3.34$ Å is added for convenience.

Figure 5 shows the corrugation against sliding for armchair and zigzag nanotubes. Our potential with locally defined normals (registry-dependent potential one, or RDP1) performs much better than the standard Lennard-Jones treatment, with a remarkably consistent overestimation of the corrugation. The overestimate may be caused by curvature-induced rehybridization of orbitals,[34] angular dependence not captured by Eq. (3), or the means of defining the normals. The semilocal normals (RDP2) with $a=0.167$ are close to the radial direction even in small-diameter nanotubes. The RDP2 results are in better overall agreement with the LDA data, although RDP1 maintains a more consistent behavior.[35]

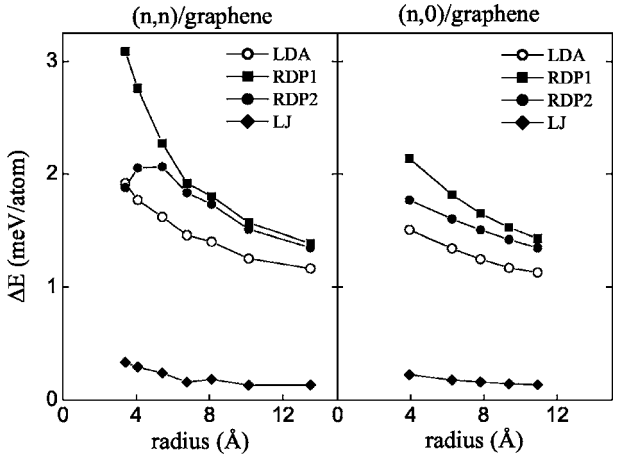

FIG. 5. Corrugation against sliding for the nanotube/substrate interaction per atom of nanotube. The nanotubes are positioned 3.2 Å above a graphitic substrate; the energy difference is evaluated for structures when the lowest row of atoms on the nanotube is in *AA* or *AB* registration with the graphene layer. Armchair nanotubes, from left to right: (5,5), (6,6), (8,8), (10,10), (12,12), (15,15), (20,20); zigzag nanotubes, from left to right: (10,0), (16,0), (20,0), (24,0), (28,0).

The nanotube/nanotube tests are particularly challenging, since the corrugation under rotation and sliding is extremely small due to efficient averaging of the intertube interaction.[2,4,14,33,36] Even when nanotubes are axially commensurate, circumferential incommensuration due to difference in radii between the layers reduces the corrugation and allows a smooth relative motion of nested nanotubes.

One of the special cases, widely discussed in the literature,[14,37] is a $(5,5)/(10,10)$ system, which has short angular and axial periods. For this test we relax the (5,5) and (10,10) single-walled nanotubes individually in the LDA and keep them rigid during rotation and sliding. If the system starts from the most symmetric alignment[37] the maximum corrugation in our simulations is achieved when one of the nanotubes is shifted by $\sqrt{3}/4a_0$ along the axis or rotated by $\pi/20$ around the axis of the double-walled nanotube. Our LDA corrugation, shown in Table I, is lower than that

TABLE I. Corrugation against sliding and rotation in meV per unit cell of a double walled nanotube (DWNT) (60, 108, 76 atoms, respectively).

DWNT	Motion	LDA	RDP2	RDP1	RDP0	LJ
(5,5)/(10,10)	Slide	<1	3	28	20	−0.3
	Rotate	18	19	−98	55	−1.0
(9,0)/(18,0)	Slide	−109	−186	−176	−280	−13
	Rotate	<1	13	35	36	<0.1
(7,7)/(12,12)	Slide	<1	6	6	48	−0.4

TABLE II. The equilibrium interlayer spacing for different allotropic forms of graphite. The theoretical value for turbostratic graphite, calculated with the RDP1, is in much better agreement with experiment than the value produced by the LJ potential (Ref. 40). Experimental data is not available for AA stacking.

Stacking	LJ	RDP1	Expt.
AB	3.340	3.34	3.34 (Ref. 15)
Turbostratic	3.349	3.43	3.44 (Ref. 39).
AA	3.368	3.57	

calculated previously (i.e., 14 meV for sliding and 31 meV for rotation[37]). We attribute this discrepancy to the very small size of the corrugation (less than 1 meV/atom), which makes the results very sensitive to details of calculations, such as the choice of pseudopotential and convergence criteria.[38] If, for example, we use a lower energy cutoff of 287 eV in our soft-pseudopotential calculations, the corrugation against sliding in the $(5,5)/(10,10)$ system changes to -15 meV per unit cell. For comparison, the energy difference between *AA* and *AB* stacking of graphite (which does not suffer from this geometrical cancellation) changes by just 3% (0.5 meV per atom) when the cutoff is reduced from 358 to 287 eV. For all double-walled nanotubes studied, nine special points along the axis provided good *k*-point convergence. In other multilayer tubes with longer axial or angular periodicity (or quasiperiodicity), the geometrical cancellation is so effective that the corrugation is essentially zero within the limits of accuracy of most theoretical methods: in these systems, it is the geometry (and for some properties, local distortions) that sets the overall corrugation-related interlayer behavior of uniform systems, not simply the very smooth global energetics of the corrugated potential. RDP2 adequately describes the qualitative distinction between the relatively large corrugation for $(5,5)/(10,10)$ and $(9,0)/(18,0)$ tubes and the much smaller corrugation (under 0.1 meV/atom) of less symmetric tubes such as $(7,7)/(12,12)$, as shown in Table I.

The registry dependence in our interlayer potential has been trained and tested on theoretical results for corrugation in graphitic structures. However, the equilibrium interlayer spacing in turbostratic graphite provides an independent experimental test of the potential. The layers of turbostratic graphite are randomly rotated with respect to one another, so the atoms in different layers assume essentially all possible registrations. Therefore one expects the equilibrium interlayer distance to be greater than that of *AB* stacking and less than that of the least favorable ordered stacking, *AA*. In fact, the experimental spacing for turbostratic graphite is 3.44 Å.[39]

We calculated the equilibrium interlayer spacing for these three forms of graphite with the Lennard-Jones potential[40] and with the RDP (RDP1 and RDP2 are identical for a flat surface). As shown in Table II, the RDP spacing matches the experimental value very well. The near-perfect agreement suggests that the averaging within turbostratic stacking is insensitive to detailed characteristics of the potential used, so long as the overall magnitude of the corrugation is correct.

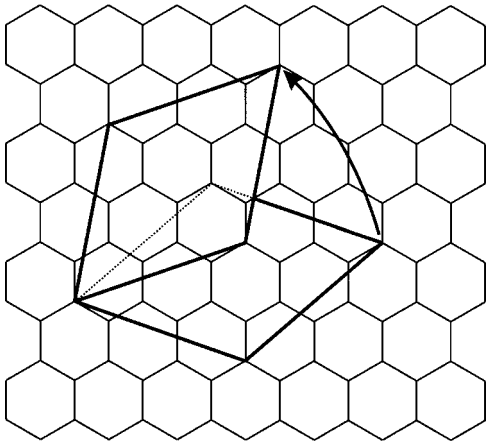

FIG. 6. An example of accidental commensuration in graphite. The two layers become commensurate when rotated by $\cos^{-1}(11/14)$ with respect to each other. The resulting skewed unit cell has 14 atoms in each layer.

The RDP was not fitted to the experimental turbostratic data (in fact, we were unaware of these data when designing the potential). As expected, the LJ treatment of turbostratic stacking is much too smooth, with very little dilation compared to the optimal *AB* stacking.

We can simulate turbostratic stacking within the LDA by using a skewed supercell configuration of graphene bilayers.[41] These accidental angular commensurations can be produced by constructing supercells using spatially inverted supercell vectors such as (4,1) and (1,4), as shown in Fig. 6. The bilayer supercell contains 14+14 atoms, with the two layers rotated by $\cos^{-1}(11/14)$ with respect to each other. The energy of the mismatched system at 3.34 Å spacing is 3.6 meV/atom higher than that of the *AB* stacking and the corrugation against sliding is very small. Similar behavior (a 3.4 meV/atom increase) occurs in a larger structure with a (26+26)-atom supercell and $\cos^{-1}(11/13)$ mismatch. [To our knowledge, these are the first density functional theory (DFT) calculations on supercell analogs to turbostratic graphite.] The RDP gives an increase of 5.2 and 4.9 meV/atom above optimal stacking for the two cases, respectively, and practically no corrugation against sliding. Even in these relatively small supercells the interlayer interaction averages out efficiently to obtain a mean binding energy.

In summary, we show that, although the absolute cohesion is not properly modeled in the local DFT approximations, the corrugation against sliding appears to be more accurate than previously suspected. Combining these results with experimental data for the interlayer spacing, compressibility, and exfoliation energy, we construct an empirical registry-dependent potential which is much more accurate than the Lennard-Jones potential for describing the corrugation in interlayer interactions in graphene nanostructures.[42]

We thank Paul Lammert and Jorge Sofo for valuable discussions. We also gratefully acknowledge the National Science Foundation support through Grant No. DMR-0305035.

[1] S. Iijima, Nature (London) **354**, 56 (1991).
[2] J. Cummings and A. Zettl, Science **289**, 602 (2000).
[3] A. M. Fennimore, T. D. Yuzvinsky, W. Q. Han, M. S. Fuhrer, J. Cumings, and A. Zettl, Nature (London) **424**, 408 (2003).
[4] M.-F. Yu, B. I. Yakobson, and R. S. Ruoff, J. Phys. Chem. B **104**, 8764 (2000).
[5] Yu. E. Lozovik, A. V. Minogin, and A. M. Popov, Pis'ma Zh. Eksp. Teor. Fiz. **77**, 759 (2003).
[6] A. Buldum and J. P. Lu, Phys. Rev. Lett. **83**, 5050 (1999).
[7] A. N. Kolmogorov, V. H. Crespi, M. H. Schleier-Smith, and J. C. Ellenbogen, Phys. Rev. Lett. **92**, 085503 (2004).
[8] L. A. Girifalco and M. Hodak, Phys. Rev. B **65**, 125404 (2002).
[9] H. Rydberg, M. Dion, N. Jacobson, E. Schroder, P. Hyldgaard, S. I. Simak, D. C. Langreth, and B. I. Lundqvist, Phys. Rev. Lett. **91**, 126402 (2003).
[10] M. Hasegawa and K. Nishidate, Phys. Rev. B **70**, 205431 (2004).
[11] A. G. Marinopoulos, L. Reining, V. Olevano, and A. Rubio, Phys. Rev. Lett. **89**, 076402 (2002).
[12] As we discuss later in the paper, the contribution to the corrugation from the van der Waals term is expected to be insignificant.
[13] J.-C. Charlier, X. Gonze, and J. P. Michenaud, Carbon **32**, 289 (1994).
[14] A. H. R. Palser, Phys. Chem. Chem. Phys. **1**, 4459 (1999).
[15] Y. Baskin and L. Mayer, Phys. Rev. **100**, 544 (1955).
[16] R. Nicklow, W. Wakabayashi, and H. G. Smith, Phys. Rev. B **5**, 4951 (1972).
[17] L. A. Girifalco and R. A. Ladd, J. Chem. Phys. **25**, 693 (1956).
[18] L. X. Benedict, N. G. Chopra, M. L. Cohen, A. Zettl, S. G. Louie, and V. H. Crespi, Chem. Phys. Lett. **286**, 490 (1998).
[19] R. Zacharia, H. Ulbricht, and T. Hertel, Phys. Rev. B **69**, 155406 (2004).
[20] The experimental values also include subtle thermal effects (Ref. 10).
[21] G. Kresse and J. Hafner, Phys. Rev. B **47**, R558 (1993).
[22] G. Kresse and J. Hafner, Phys. Rev. B **49**, 14251 (1994).
[23] G. Kresse and J. Furthmuller, Comput. Mater. Sci. **6**, 15 (1996).
[24] G. Kresse and J. Furthmuller, Phys. Rev. B **54**, 11169 (1996).
[25] D. Vanderbilt, Phys. Rev. B **41**, R7892 (1990).
[26] D. M. Ceperley and B. J. Alder, Phys. Rev. Lett. **45**, 566 (1980); J. P. Perdew and A. Zunger, Phys. Rev. B **23**, 5048 (1981).
[27] J. P. Perdew, K. Burke, and M. Ernzerhof, Phys. Rev. Lett. **77**, 3865 (1996).
[28] J. D. Pack and H. J. Monkhorst, Phys. Rev. B **13**, 5188 (1976); **16**, 1748 (1977).
[29] N. Troullier and J. L. Martins, Phys. Rev. B **43**, 1993 (1991).
[30] P. E. Blochl, Phys. Rev. B **50**, 17953 (1994).
[31] L. A. Girifalco, M. Hodak, and R. S. Lee, Phys. Rev. B **62**, 13104 (2000).
[32] A. D. Crowell and J. S. Brown, Surf. Sci. **123**, 296 (1982).
[33] A. N. Kolmogorov and V. H. Crespi, Phys. Rev. Lett. **85**, 4727 (2000).
[34] T. Dumitrica, C. M. Landis, and B. I. Yakobson, Chem. Phys. Lett. **360**, 182 (2002).
[35] For this reason, we used the local definition of the normals in our study of the nanotube/graphite interaction (Ref. 7) so that the comparison of alignment effects for tubes of different diameters and helicities has a consistent degree of accuracy.
[36] M. Damnjanović, I. Milošević, T. Vuković, and R. Sredanović, Phys. Rev. B **60**, 2728 (1999); T. Vuković, M. Damnjanović, and I. Milošević, Physica E (Amsterdam) **16**, 259 (2003).
[37] J.-C. Charlier and J.-P. Michenaud, Phys. Rev. Lett. **70**, 1858 (1993).
[38] Since these barriers are very sensitive to subtle geometrical effects, nonidealities in real structures due to, e.g., external perturbations or thermal broadening could change the rotational and translational barriers. Therefore these results should be considered as a test of the classical potentials against an important representative double-walled structure, not as calculations of actual rotational or translational barriers under real (i.e., nonideal) experimental conditions.
[39] C. H. Kiang, M. Endo, P. M. Ajayan, G. Dresselhaus, and M. S. Dresselhaus, Phys. Rev. Lett. **81**, 1869 (1998); V. Bayot, L. Piraux, J. P. Michenaud, J. P. Issi, M. Lelaurain, and A. Moore, Phys. Rev. B **41**, 11770 (1990).
[40] We are interested in the change in the equilibrium spacing, so for convenience, we slightly adjusted the LJ potential parameters to have the equilibrium spacing of *AB* stacking at exactly 3.34 Å.
[41] H. Beyer, M. Muller, and Th. Schimmel, Appl. Phys. A: Mater. Sci. Process. **68**, 163 (1999).
[42] Since our potential is classical, it does not embody long-ranged, low-energy quantum effects which may, for example, perturb the low-energy band structure of a graphene sheet due to its interaction with scattering centers (such as vacancies or nanotubes) which rest on or in the surface.